

Formation of HHgC_2H_5 in the Hg-Sensitized Photolysis of $\text{H}_2/\text{C}_2\text{H}_4$ Mixtures

C. Kerst, I. Lein, P. Potzinger,* and H. G. Wagner

Max-Planck-Institut für Strömungsforschung, Bunsenstrasse 10, 37073 Göttingen, Germany

Received: August 30, 1996; In Final Form: March 11, 1997[⊗]

In the Hg-sensitized photolysis of H_2 in the presence of C_2H_4 the sensitizer Hg is consumed under formation of a metastable compound. The rate of formation and the steady-state concentration of this compound have been studied as a function of Hg, H_2 , and C_2H_4 concentration, absorbed light intensity, temperature, and in the presence of radical scavengers. All these experiments ask for the participation of HgH and C_2H_5 in the formation of the Hg compound. We therefore suggest that these two radicals combine under formation of HHgC_2H_5 . Further support comes from two color photolysis experiments where HgH and C_2H_5 radicals have been generated independently. HHgC_2H_5 decomposes under 206 nm irradiation and much slower in the dark. It is also very easily attacked by radicals.

Introduction

Mercury atoms excited to the $^3\text{P}_1$ state may undergo an energy transfer to, or a photoreaction with, a substrate molecule, depending on the chemical nature of the substrate. If the substrate provides a suitable state which accepts the energy, an energy transfer will occur. Otherwise a photoreaction will take place which can be further subdivided into metathetical and addition reactions.¹ A typical example of an energy-transfer reaction is the reaction of $\text{Hg}(^3\text{P}_1)$ with *cis*-butene leading to a *cis*–*trans* isomerization.² The reaction of $\text{Hg}(^3\text{P}_1)$ with H_2 is a well-known example of a metathetical reaction.³ The HgH formed in this photoreaction has a low bond dissociation energy⁴ and leads to a fast collisionally induced decomposition which restores the original Hg concentration.⁵ In other cases, such as the reaction of $\text{Hg}(^3\text{P}_1)$ with oxides, chlorides, or sulfides, stable mercury compounds are formed.⁶ Pimentel and co-workers⁷ have shown that $\text{Hg}(^3\text{P}_1)$ atoms insert into the C–Cl bond of a chloride, and the addition product was observed in a matrix at low temperature. A very detailed account of the reaction mechanism of excited Hg atoms with H_2 , the C–H and Si–H bond has recently been given by Breckenridge.⁸

With the exceptions mentioned above, it is always assumed that in Hg-sensitized gas-phase reactions Hg atoms are regenerated very quickly independent of the type of reaction they undergo. Surprisingly, in the case of the Hg-sensitized photolysis of Me_3SiH a moderately stable mercury compound is formed.⁹ Further experiments showed that this phenomenon is not limited to silanes but can also be observed with other classes of substrates.¹⁰

Here we report the Hg-sensitized photolysis of H_2 in the presence of ethylene leading to the removal of Hg. We discuss our attempts to unravel the nature of the metastable Hg compound, as well as the pathways leading to its formation.

Experimental Section

All substances were of commercial origin and used without further purification. Azoethane contained a large ethanol impurity.

Gas handling was performed on a conventional vacuum line. Reactant pressures were determined by capacitance manometers

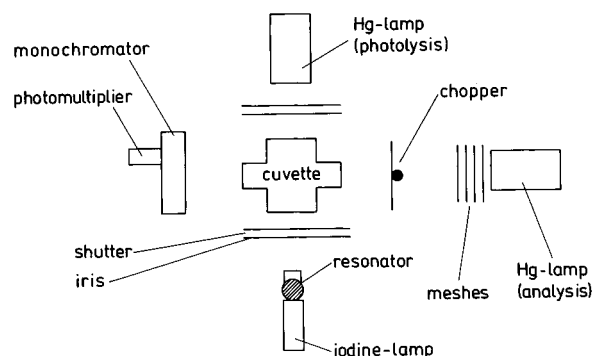


Figure 1. Experimental setup of the two color photolysis experiments.

(MKS Baratron 220 and 122A). The Hg concentration was determined by an absorption experiment.

Some of the photolysis experiments were carried out as described in ref 9, the low-pressure Hg lamp acted as photolysis source as well as analysis lamp. Photolysis experiments were performed at room, elevated, and low-temperatures. In the low temperature setup we used a double-walled cuvette thermostated by a cryostat (Lauda, RM6T).

In another series of experiments we carried out two color photolysis experiments as shown in Figure 1. The reaction mixture was photolyzed by a low-pressure Hg lamp ($\lambda = 254$ nm) and/or by a microwave driven iodine lamp ($\lambda = 206$ nm). The second low pressure Hg-arc served as an analysis lamp. The intensity of the monitoring light was attenuated by wire meshes to avoid photochemical reactions. The monitoring light, modulated by a chopper (HMS 220), passed the cuvette at right angle to the photolyzing light, was dispersed by a monochromator and detected by a photomultiplier. The signal was amplified by a lock-in amplifier (Ithaco Dynatrac 399) and finally recorded.

The intensity of the low-pressure Hg-lamps was determined by *cis*-butene ($\Phi(\text{trans-butene}) = 0.5^{11}$) as well as N_2O ($\Phi(\text{N}_2) = 1.0^{12}$) actinometry. The values of the two actinometers agreed within 1.6%. The intensity of the iodine lamp was determined by HBr-actinometry ($\Phi(\text{H}_2) = 1.0^{13}$).

Endproduct analyses by GC and MS were performed as described in ref 14.

The conversion of Hg-resonance radiation absorption values into Hg-concentration values was determined through the use of calibration plots described in ref 10.

[⊗] Abstract published in *Advance ACS Abstracts*, April 15, 1997.

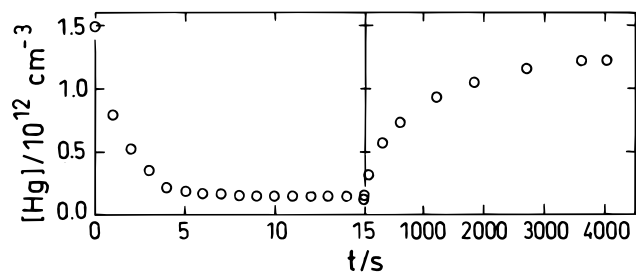


Figure 2. Change of the Hg concentration as a function of time (a) 254 nm light on and (b) 254 nm light off (exp 16, Table 1).

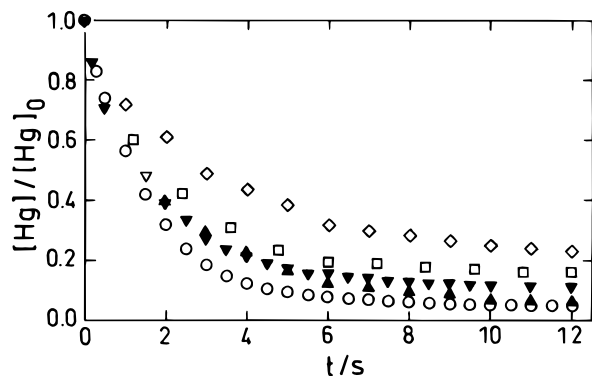


Figure 3. Change of the Hg concentration as a function of time for different initial Hg concentrations (exp 1 (○), 2 (▼), 3 (□), 4 (▲), 5 (◇), Table 1).

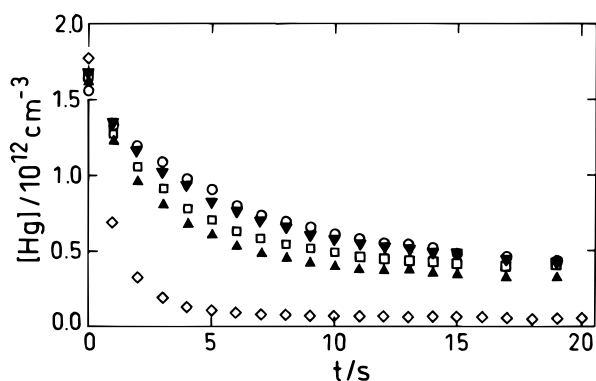


Figure 4. Change of the Hg concentration as a function of time for different 254 nm light intensities (exp 6 (○), 7 (▼), 8 (□), 9 (▲), 10 (◇), Table 1).

Results

Hg-sensitized photolysis of H_2 in the presence of C_2H_4 results in an almost complete loss of Hg. The Hg-concentration recovers quite slowly when the resonance radiation is shut off (Figure 2). A metastable mercury compound X must be formed which does not absorb at all or only weakly at 254 nm. Hg-sensitized photolysis of pure C_2H_4 or pure H_2 does not result in any reduction of the Hg-concentration. The rate of Hg-removal and to a lesser extent the stationary Hg-concentration depends on the initial Hg-concentration, light intensity, H_2 -concentration, and temperature. The rate of Hg-disappearance increases with increasing initial Hg-concentration (Figure 3). This is also observed for the absorbed intensity of the Hg-resonance radiation (Figure 4). H_2 inhibits the formation of X to such an extent, that its formation comes to an almost complete halt at high H_2 pressure (Figure 5). The temperature was varied between -1.5°C and 100°C and had a large effect on the formation of X, i.e., it decreased with increasing temperature and was almost negligible at 100°C (Figure 6). The experiments were repeated after a dark period in which the Hg-

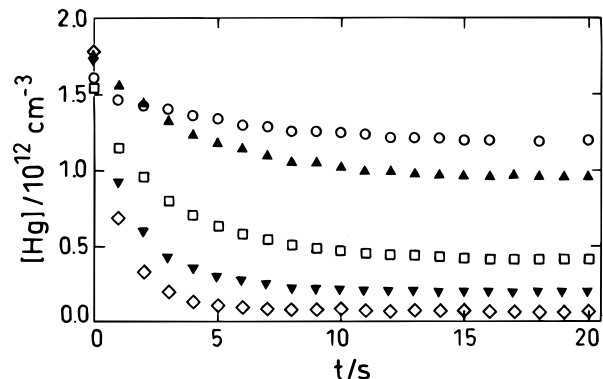


Figure 5. Change of the Hg concentration as a function of time for different H_2 concentrations (exp 11 (○), 12 (▲), 13 (□), 14 (▼), 15 (◇), Table 1).

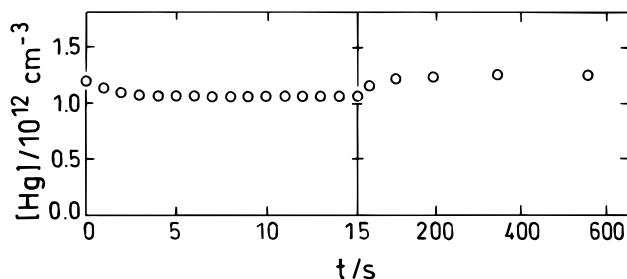


Figure 6. Change of the Hg concentration as a function of time at 373 K: (a) 254 nm light on and (b) 254 nm light off (exp 20, Table 1).

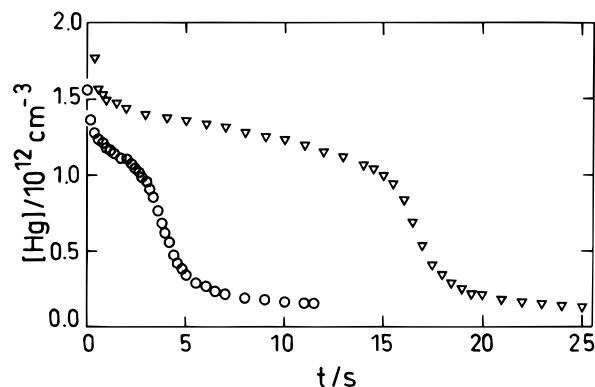
concentration recovered to its original value. The reproducibility can be seen from the two values given for α and β in Table 1, experiments 16–20. Adding O_2 to the reaction mixture inhibits the disappearance of Hg until all the O_2 has reacted (Figure 7). Similar results were obtained with NO .¹⁰ Changing the C_2H_4 -concentration by a factor of almost one hundred had only a very minor effect (Figure 8). The mercury concentration – time profiles shown in Figure 3 may be the result of the change in the Hg-concentration and/or the change in the absorbed light intensity. To check specifically the influence of ground-state mercury concentration on the formation of X, the following experiment was performed: Change in the Hg-concentration is accompanied by a change in the absorbed light intensity, therefore the incident light was adjusted so that the absorbed light intensity was kept constant, at least at the beginning of the photolysis (Figure 9). All the experiments reported so far were carried out with the simple one lamp arrangement of.⁹ Experimental details are given in Table 1.

To elucidate the reaction paths leading to the metastable Hg-compound other sources of H-atoms and radicals were utilized. The photolysis of NH_3 at 206 nm was used as an alternative H-atom source. The primary step is the formation of an H-atom and a NH_2 -radical.¹⁵ Similarly, azoethane was used as an alternative ethyl-radical source. Photolysis of pure Et_2N_2 at 206 nm produced mainly N_2 and C_4H_{10} , as well as small amounts of C_2H_6 , C_2H_4 and C_3H_8 . Reactant concentrations, experimental conditions, and results are compiled in Table 2 and Table 3.

When the reaction mixture $\text{Hg}/\text{H}_2/\text{C}_2\text{H}_4/\text{NH}_3$ was photolyzed at 206 nm, no decrease in the Hg concentration was observed (Table 2, exp 33). Photolysis of the above mixture at 254 nm radiation leads to the known almost complete disappearance of Hg. Upon irradiation with both wavelengths, 206 and 254 nm, an increase of the stationary Hg concentration is observed (Figure 10). In a similar experiment the same reaction mixture was photolyzed by 254 nm light until the stationary Hg

TABLE 1: Experimental Conditions and Results of the 254 nm Photolysis of Hg/H₂/C₂H₄/O₂/Mixtures

| exp | [Hg]/10 ¹² cm ⁻³ | [C ₂ H ₄]/10 ¹⁵ cm ⁻³ | [H ₂]/10 ¹⁸ cm ⁻³ | [O ₂]/10 ¹⁴ cm ⁻³ | I ₀ /10 ¹³ cm ⁻³ s ⁻¹ | T/K | results | α/10 ⁻¹ | β/10 ⁻⁷ cm ^{3/2} s ⁻¹ |
|-----|--|--|---|---|---|-----|-------------|--------------------|--|
| 1 | 1.9 | 3.04 | 1.19 | | 3.36 | 298 | s, Figure 3 | 1.31 | 6.13 |
| 2 | 0.65 | 3.15 | 1.19 | | 3.35 | 298 | s, Figure 3 | 3.06 | 9.28 |
| 3 | 0.35 | 3.22 | 1.19 | | 3.55 | 298 | s, Figure 3 | 3.74 | 10.63 |
| 4 | 0.26 | 3.17 | 1.20 | | 3.41 | 298 | s, Figure 3 | 1.76 | 11.49 |
| 5 | 0.14 | 3.27 | 1.19 | | 3.42 | 298 | s, Figure 3 | 4.40 | 10.66 |
| 6 | 1.5 | 2.57 | 1.22 | | 0.89 | 298 | s, Figure 4 | 4.67 | 1.52 |
| 7 | 1.6 | 2.57 | 1.24 | | 1.17 | 298 | s, Figure 4 | 4.88 | 1.98 |
| 8 | 1.6 | 2.51 | 1.24 | | 1.40 | 298 | s, Figure 4 | 4.83 | 2.74 |
| 9 | 1.6 | 2.51 | 1.23 | | 1.54 | 298 | s, Figure 4 | 4.42 | 3.13 |
| 10 | 1.5 | 2.48 | 1.21 | | 3.42 | 298 | s, Figure 4 | 3.23 | 6.33 |
| 11 | 1.6 | 3.13 | 23.8 | | 3.41 | 298 | s, Figure 5 | 8.64 | 1.72 |
| 12 | 1.7 | 3.14 | 11.8 | | 3.64 | 298 | s, Figure 5 | 7.28 | 2.11 |
| 13 | 1.5 | 3.22 | 5.91 | | 3.60 | 298 | s, Figure 5 | 5.06 | 3.32 |
| 14 | 1.8 | 3.15 | 2.33 | | 3.67 | 298 | s, Figure 5 | 3.29 | 6.70 |
| 15 | 1.8 | 3.11 | 1.19 | | 3.69 | 298 | s, Figure 5 | 1.76 | 10.46 |
| 16 | 1.5 | 2.49 | 1.22 | | 3.11 | 298 | s, Figure 2 | 2.82 | 7.30 |
| | | | | | | | | 3.97 ^a | 8.07 ^a |
| 17 | 1.3 | 2.52 | 1.22 | | 3.10 | 313 | | 4.86 | 4.64 |
| | | | | | | | | 5.34 ^a | 5.26 ^a |
| 18 | 1.4 | 2.48 | 1.22 | | 3.25 | 333 | | 7.35 | 5.13 |
| | | | | | | | | 7.55 ^a | 3.92 ^a |
| 19 | 1.6 | 2.52 | 1.22 | | 3.21 | 353 | | 8.42 | 4.16 |
| | | | | | | | | 8.74 ^a | 3.75 ^a |
| 20 | 1.2 | 2.49 | 1.22 | | 3.29 | 373 | s, Figure 6 | 9.39 | 6.27 |
| | | | | | | | | 9.53 ^a | 5.04 ^a |
| 21 | 1.9 | 2.72 | 2.62 | 5.23 | 3.42 | 298 | s, Figure 7 | | |
| 22 | 1.6 | 2.71 | 2.65 | 0.34 | 3.34 | 298 | s, Figure 7 | | |
| 23 | 1.9 | 3.04 | 1.19 | | 3.36 | 298 | s, Figure 8 | | |
| 24 | 1.7 | 24.44 | 1.17 | | 4.10 | 298 | s, Figure 8 | | |
| 25 | 1.8 | 122.1 | 1.07 | | 4.16 | 298 | s, Figure 8 | | |
| 26 | 1.9 | 244.1 | 0.95 | | 4.18 | 298 | s, Figure 8 | | |
| 27 | 0.24 | 2.54 | 1.24 | | 3.00 | 298 | s, Figure 9 | 5.47 | 11.86 |
| 28 | 0.40 | 2.49 | 1.22 | | 1.63 | 298 | s, Figure 9 | 4.22 | 5.99 |
| 29 | 0.51 | 2.43 | 1.22 | | 1.43 | 298 | s, Figure 9 | 4.67 | 5.91 |
| 30 | 0.64 | 2.48 | 1.23 | | 1.14 | 298 | s, Figure 9 | 4.72 | 2.88 |
| 31 | 1.2 | 2.45 | 1.22 | | 0.86 | 298 | s, Figure 9 | 5.30 | 1.90 |
| 32 | 1.9 | 2.50 | 1.22 | | 0.70 | 298 | s, Figure 9 | 6.16 | 1.28 |

^a Experiment repeated after a dark period.**Figure 7.** Change of the Hg concentration as a function of time in the presence of O₂ (exp 21 (▽) and 22 (○), Table 1).

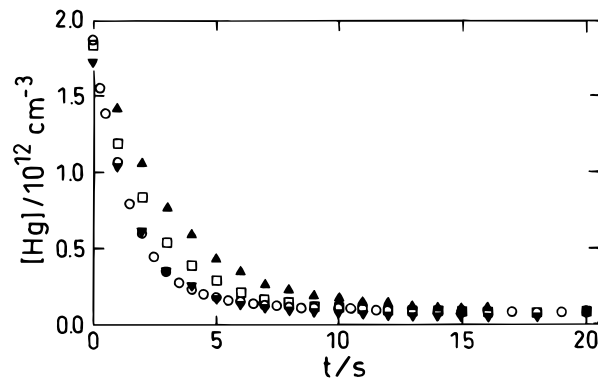
concentration was reached; then the iodine lamp was turned on. An increase in the stationary Hg concentration is observed, the extent of which depends on the intensity of the two light sources (Figure 11).

Hg-sensitized photolysis of NH₃ in the presence of C₂H₄ did not result in any Hg-removal (Table 2, exp 39, 40).

The slow increase in Hg concentration after 254 nm photolysis of a Hg/H₂/C₂H₄ mixture could be accelerated by illuminating the product mixture with 206 nm radiation (Figure 12).

Simultaneous photolysis of a Hg/Et₂N₂ mixture at 254 and 206 nm caused no loss of Hg (Table 3, exp 42).

Photolysis of a Hg/H₂/Et₂N₂ mixture at 206 nm or 254 nm had no effect on the Hg concentration, while simultaneous

**Figure 8.** Change of the Hg concentration as a function of time for different C₂H₄ concentrations (exp 23 (○), 24 (▽), 25 (□), 26 (▲), Table 1).

irradiation with light of both wavelengths resulted in a loss of Hg (Figure 13).

An attempt to characterize the metastable Hg compound by mass spectrometry failed.

The [C₂H₆]/[C₄H₁₀] ratio was determined in the photolysis of Et₂N₂ at 366 nm to be 0.124 ± 0.005, whereas in our standard system Hg/H₂/C₂H₄ at 254 nm we determined [C₂H₆]/[C₄H₁₀] = 0.16 ± 0.01.

Discussion

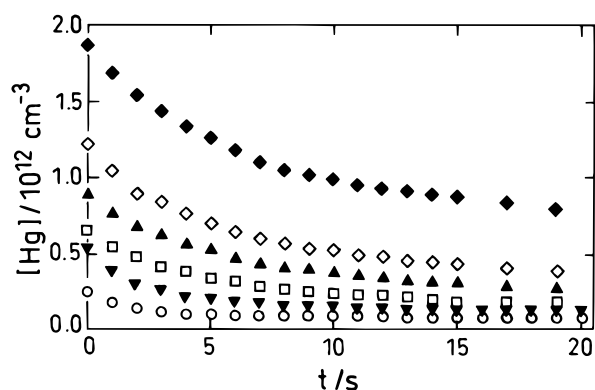
In recent publications^{16–19} it has been shown that reactions of excited metal atoms such as Mg(¹P), Zn(³P₁), and Hg(³P₁)

TABLE 2: Experimental Conditions and Results of the Photolysis of Hg/H₂/C₂H₄/NH₃ Mixtures at the Two Wavelengths 254 and 206 nm

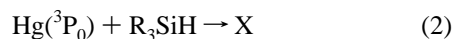
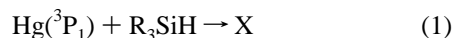
| exp | [C ₂ H ₄]/10 ¹⁵ cm ⁻³ | [NH ₃]/10 ¹⁶ cm ⁻³ | [H ₂]/10 ¹⁸ cm ⁻³ | t/s | I ₀ (λ = 254 nm)/% | I ₀ (λ = 206 nm)/% | results |
|-----|--|--|---|-------------|-------------------------------|-------------------------------|--------------|
| 33 | 4.72 | 6.34 | 1.20 | | 0 | 100 | [Hg] ≠ f(t) |
| 34 | 4.45 | 6.25 | 1.19 | 0–30.5 | 100 | 0 | s, Figure 10 |
| | | | | 30.5–661.2 | 0 | 0 | |
| 35 | 4.71 | 6.73 | 1.20 | 0–30.3 | 100 | 100 | s, Figure 10 |
| | | | | 30.3–605.6 | 0 | 0 | |
| 36 | 4.67 | 6.55 | 1.21 | 0–31.8 | 10.5 | 0 | s, Figure 11 |
| | | | | 31.8–46.8 | 10.5 | 100 | |
| 37 | 4.75 | 6.66 | 1.20 | 0–25.4 | 52.6 | 0 | s, Figure 11 |
| | | | | 25.4–40.3 | 52.6 | 100 | |
| 38 | 4.66 | 6.37 | 1.20 | 0–25.1 | 100 | 0 | s, Figure 11 |
| | | | | 25.1–40.0 | 100 | 100 | |
| 39 | 4.66 | 24.76 | 0 | | 100 | 0 | [Hg] ≠ f(t) |
| 40 | 4.72 | 74.29 | 0 | | 100 | 0 | [Hg] ≠ f(t) |
| 41 | 4.69 | 0 | 1.19 | 0–30.2 | 100 | 0 | s, Figure 12 |
| | | | | 30.2–115.2 | 0 | 0 | |
| | | | | 115.2–220.5 | 0 | 100 | |

TABLE 3: Experimental Conditions and Results of the Photolysis of Hg/H₂/Et₂N₂ Mixtures at the Two Wavelengths 254 and 206 nm

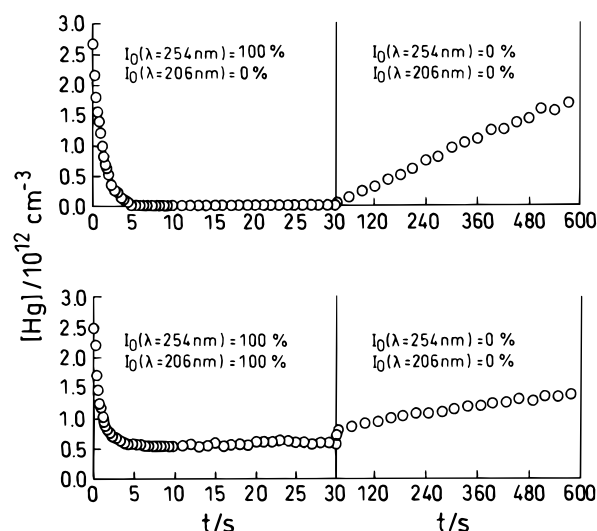
| exp | [Et ₂ N ₂]/10 ¹⁶ cm ⁻³ | [H ₂]/10 ¹⁸ cm ⁻³ | t/s | I ₀ (λ = 254 nm)/% | I ₀ (λ = 206 nm)/% | results |
|-----|---|---|------------|-------------------------------|-------------------------------|--------------|
| 42 | 9.50 | 0 | 0–28.2 | 100 | 100 | [Hg] ≠ f(t) |
| 43 | 9.89 | 1.19 | 0–10.0 | 0 | 100 | s, Figure 13 |
| | | | 10.0–39.5 | 100 | 100 | |
| | | | 39.5–73.5 | 0 | 100 | |
| | | | 73.5–423.9 | 0 | 0 | |

**Figure 9.** Change of the Hg concentration as a function of time for different Hg concentrations under the condition of constant absorbed light intensity (exp 27 (○), 28 (▼), 29 (□), 30 (▲), 31 (◇), 32 (◆), Table 1).

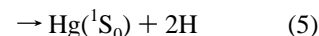
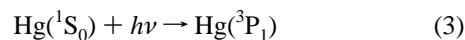
with H₂ and CH₄ in a solid matrix result in the formation of MgH₂, ZnH₂, HgH₂, HMgCH₃, and HHgCH₃. It is suggested²⁰ that these compounds are formed by direct insertion of the excited metal atom into the H–H and C–H bond, respectively. A similar mechanism was discussed in the Hg-sensitized photolysis of silanes⁹ as a possible explanation for the formation of the unknown Hg containing product X, namely, the addition of excited mercury atoms to the substrate:



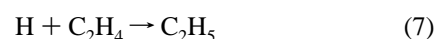
These reactions can be immediately discarded in the Hg-sensitized photolysis of the H₂/C₂H₄ mixture. The Hg(³P₁) is quenched predominantly by H₂ under our experimental conditions, and no decrease of the Hg concentration was observed in a Hg/H₂ (or a Hg/C₂H₄) system. The mechanism of the Hg-sensitized photolysis of H₂ has been carefully studied by Callear

**Figure 10.** Hg concentration–time profiles in the two color photolysis of Hg/H₂/C₂H₄/NH₃ mixtures and in the dark periods (exp 34, 35, Table 2).

and co-workers,³ and the mechanism is as follows:



The H atoms are scavenged by C₂H₄:



It seems therefore likely that H atoms and/or ethyl radicals are involved in the formation of the metastable compound X. These

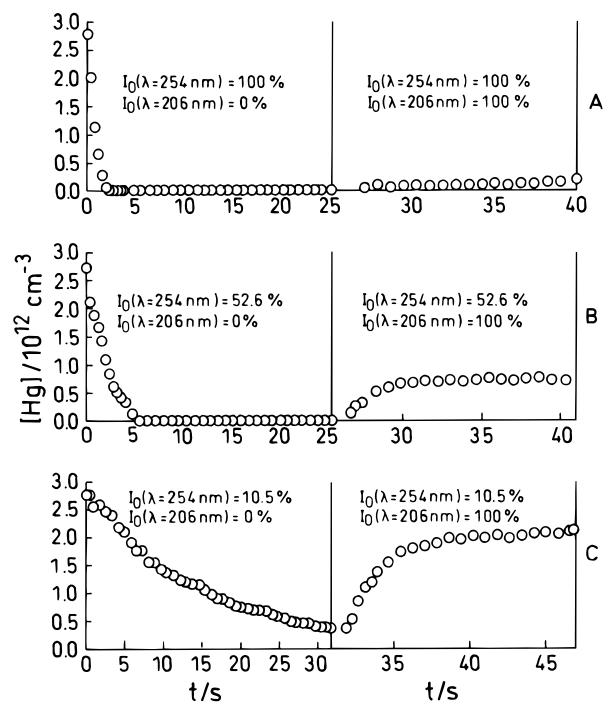


Figure 11. Decomposition of the Hg compound by 206 nm irradiation in the 254 nm photolysis of a Hg/H₂/C₂H₄/NH₃ mixture (exp 36–38, Table 2).

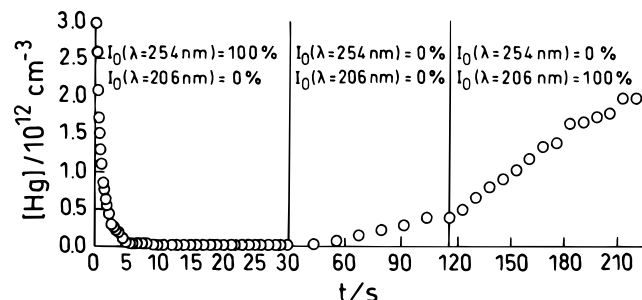


Figure 12. Dependence of the lifetime of the Hg compound on 206 nm irradiation (exp 41, Table 2).

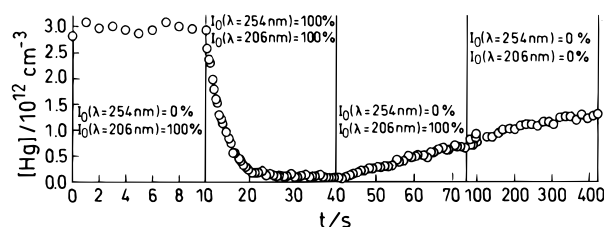
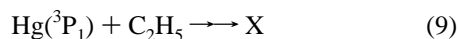
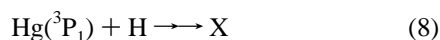


Figure 13. Dependence of the rate of formation and rate of decomposition of the Hg compound on the wavelength in the two color photolysis experiments of Hg/H₂/Et₂N₂ mixtures (exp 43, Table 3).

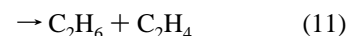
considerations are supported by the observation that typical radical scavengers such as O₂ and NO inhibit the formation of X.

In the following experiments we examined which of the Hg species Hg(³P₁), Hg(³P₀), Hg(¹S₀), and HgH and which of the reactive species H and C₂H₅ are responsible for the formation of X and the removal of Hg.

The reaction of Hg(³P₁) with either H or C₂H₅ as the rate-determining step in the formation of X



can be dismissed for the reasons given below. The stationary concentrations of Hg(³P₁), C₂H₅, and H, given approximately by $[\text{Hg}(\text{}^3\text{P}_1)]_{\text{ss}} \approx I_{\text{abs}}/\{(k_4 + k_5 + k_6)[\text{H}_2]\}$, $[\text{C}_2\text{H}_5]_{\text{ss}} \approx \{2I_{\text{abs}}/(k_{10} + k_{11})\}^{1/2}$, and $[\text{H}]_{\text{ss}} \approx 2I_{\text{abs}}/k_7[\text{C}_2\text{H}_4]$ have the following values under the conditions of experiment 1: $[\text{Hg}(\text{}^3\text{P}_1)]_{\text{ss}} \approx 10^5 \text{ cm}^{-3}$, $[\text{C}_2\text{H}_5]_{\text{ss}} \approx 10^{12} \text{ cm}^{-3}$ and $[\text{H}]_{\text{ss}} \approx 10^{10} \text{ cm}^{-3}$. Even if we assume the rate of reactions 8 and 9 to be collision controlled, it would take orders of magnitude longer to build up X than is experimentally observed. These considerations are in agreement with exp 42 where Hg(³P₁) and ethyl radicals were generated by two independent light sources. Reactions 10 and 11 describe two important reactions of C₂H₅:



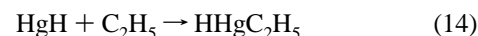
A similar calculation for Hg(³P₀) predicts an even smaller stationary concentration for Hg(³P₀) than for Hg(³P₁). The rate of formation of Hg(³P₀) is more than a factor of 30 smaller than for Hg(³P₁), outweighing the 1 order of magnitude smaller rate constant for Hg(³P₀) with H₂.²¹ This calculation is supported by an experiment in which excited Hg atoms react with NH₃ in the presence of C₂H₄. The following two reactions occur:



The H atoms are scavenged by C₂H₄ (reaction 7). In this system similar stationary concentrations of H and C₂H₅ are generated as in our standard system; in this case, however, the Hg(³P₀) stationary concentration is larger. No removal of Hg was observed in these experiments.

In a previous publication⁹ it has been proposed that the reaction of ground-state mercury atoms with radicals is the crucial step in the formation of X. Two experiments argue against such an explanation. The initial rate of Hg removal as a function of Hg concentration at constant absorbed light intensity (Figure 9) does not show the 1.5 order dependence on light intensity which one would expect if the reaction of Hg with C₂H₅ is the rate determining step in the formation of X. Experiment 33 shows that mercury atoms in the ground state and C₂H₅ radicals do not react to form X.

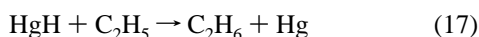
This leaves us with HgH. Indeed, if we look through Tables 2 and 3 Hg removal is observed only in the presence of HgH. In Figure 13 it is quite clearly demonstrated that besides HgH, C₂H₅ radicals have to be present to form the Hg compound under investigation. We suggest that X is formed by the combination reaction



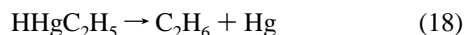
Thus, the overall mechanism of the Hg-sensitized photolysis of H₂ in the presence of C₂H₄ is made up of reactions 3–5, 7, 10, and 11 as the main steps. Furthermore it is known that HgH decomposes in a collision-induced process:²²



For M = H₂, the main collision partner in our system, the rate constant is known.²² It has been suggested by Callear et al.²³ that HgH is also attacked by H atoms and radicals in the manner of an abstraction reaction:



We now add reaction 14 to this mechanism. HHgC_2H_5 is not stable and decomposes slowly in the dark and rather quickly under irradiation. This can be accounted for by a unimolecular step



and by abstraction processes with the radicals present. If only C_2H_4 is present besides Hg and H_2 the abstraction pathway will be dominated by C_2H_5 :



In the presence of other substances, e.g., NH_3 , other radicals such as NH_2 will undergo a reaction equivalent to (19). HgC_2H_5 radicals are not characterized in the literature and are thought to have a very small bond dissociation energy²⁴ so that a fast further decomposition is quite likely:



To account for our experimental results we have to assume that reaction 15 is the main process for the destruction of HgH . Hence, the rate of Hg disappearance should be inhibited by H_2 . There should also be a temperature and intensity dependence. Reaction 15 has an appreciable activation energy²² and it will therefore be favored over reaction 14 at higher temperatures. The intensity dependence arises from the different orders in the radical concentration in reaction 14 and 15.

A more quantitative comparison is possible by examining the integrated rate equation for HHgC_2H_5 :

$$R(\text{HHgC}_2\text{H}_5) = -R(\text{Hg}) = k_{14}[\text{HgH}][\text{C}_2\text{H}_5] - k_{19}[\text{C}_2\text{H}_5]\{[\text{Hg}]_0 - [\text{Hg}]\} \quad (\text{I})$$

For HgH and C_2H_5 approximate steady-state expressions will be inserted:

$$[\text{HgH}]_{\text{ss}} \approx \frac{k_4}{k_4 + k_5} \frac{I_{\text{abs}}}{k_{15}[\text{M}]} \approx \frac{k_4}{k_4 + k_5} \frac{\kappa I_0}{k_{15}[\text{M}]} [\text{Hg}] \equiv A[\text{Hg}] \quad (\text{II})$$

$$[\text{C}_2\text{H}_5]_{\text{ss}} \approx \left(\frac{k_4 + 2k_5}{k_4 + k_5} \frac{I_{\text{abs}}}{2(k_{10} + k_{11})} \right)^{1/2} \approx \left(\frac{k_4 + 2k_5}{k_4 + k_5} \frac{\kappa I_0}{2(k_{10} + k_{11})} \right)^{1/2} [\text{Hg}]^{1/2} \equiv B[\text{Hg}]^{1/2} \quad (\text{III})$$

In the two expressions II and III it has been assumed that the absorbed light intensity I_{abs} [$\text{cm}^{-3} \text{s}^{-1}$] can be approximated by $\kappa I_0[\text{Hg}]$, where κ [cm^3] is the product of the absorption cross section σ of Hg atoms for 254 nm resonance radiation and the optical path length d . I_0^*d is the light intensity [$\text{cm}^{-2} \text{s}^{-1}$] at the entrance window of the cuvette.

We obtain the following expression for the mercury concentration as a function of time:

$$[\text{Hg}] = [\text{Hg}]_0 \alpha^2 \left(1 - \frac{2(\alpha - 1)}{(\alpha + 1) \exp([\text{Hg}]_0^{1/2} \alpha \beta t) + \alpha - 1} \right)^2 \quad (\text{IV})$$

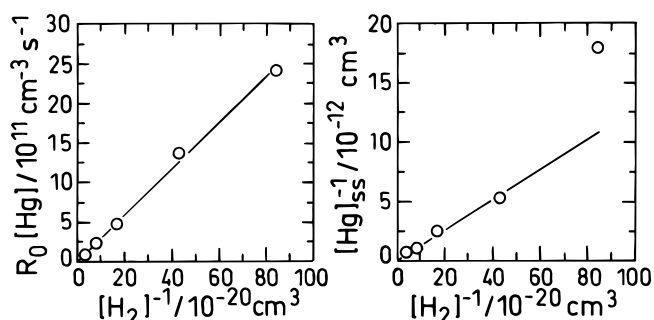


Figure 14. Dependence of the initial reaction rate and the steady-state concentration of Hg on the reciprocal H_2 concentration.

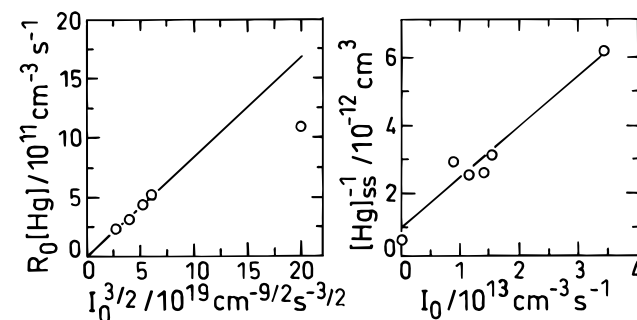


Figure 15. Dependence of the initial reaction rate and the steady-state concentration of Hg on the 254 nm absorbed light intensity.

with

$$\alpha = \left(\frac{k_{19}B}{k_{14}AB + k_{19}B} \right)^{1/2} \quad (\text{V})$$

$$\beta = k_{14}AB + k_{19}B \quad (\text{VI})$$

$[\text{Hg}]_0$ and t denote the initial mercury concentration and time, respectively. Expression IV was fitted to our experimental $[\text{Hg}]$ versus time curves with α and β as parameters. These parameters are also given in Table 1.

The initial rate R_0 of the Hg reaction is given by

$$R_0(\text{Hg}) = \lim_{t \rightarrow 0} d(\text{Hg})/dt = \beta(\alpha^2 - 1)[\text{Hg}]_0^{3/2} - \text{const} \frac{I_0^{3/2}[\text{Hg}]_0^{3/2}}{[\text{M}]} \quad (\text{VII})$$

The stationary Hg-concentration $[\text{Hg}]_{\text{ss}}$ is given by

$$[\text{Hg}]_{\text{ss}} = \alpha^2[\text{Hg}]_0 = [\text{Hg}]_0 \frac{[\text{M}]}{\text{const} I_0 + [\text{M}]} \quad (\text{VIII})$$

Equations VII and VIII express the quantitative dependence of initial rate and stationary Hg concentration on H_2 concentration, light intensity, and initial Hg concentration.

The dependence of $R_0(\text{Hg})$ and $[\text{Hg}]_{\text{ss}}$ on $[\text{H}_2]$ are depicted in Figure 14, and in both cases a straight line is obtained as predicted by the mechanism. The data point for the smallest H_2 concentration in the $1/[\text{Hg}]_{\text{ss}}$ vs $1/[\text{H}_2]$ plot is in error due to the very small Hg concentration (Figure 5).

The dependence of the initial rate on light intensity shows the expected order of $3/2$ but only at the low intensity experiments. The experimental data in the plot $1/[\text{Hg}]_{\text{ss}}$ vs I_0 are quite scattered; however, in a linear fit we obtain an intercept which agrees quite well with the value of $1/[\text{Hg}]_0$, predicted by the mechanism (Figure 15).

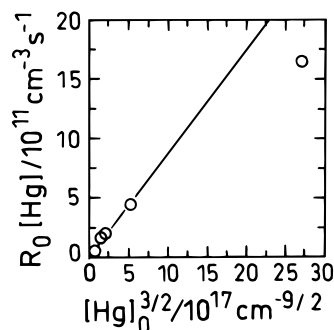


Figure 16. Dependence of the initial reaction rate of Hg on the 3/2 power of the initial Hg concentration.

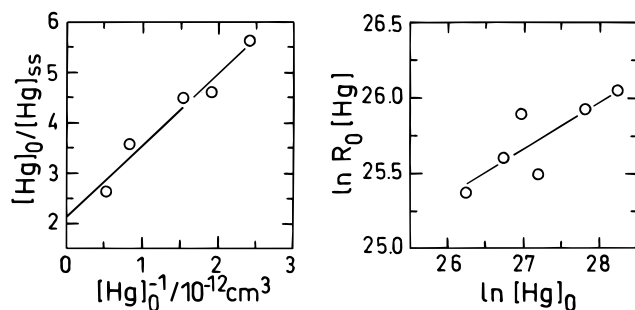


Figure 17. (a) Dependence of the reciprocal steady-state Hg concentration on the reciprocal initial Hg concentration. (b) Double-logarithmic plot of initial reaction rate of Hg on the initial Hg concentration.

The dependence on the initial mercury concentration can only be evaluated for $R_0(\text{Hg})$. The stationary Hg concentrations are quite small (Figure 3) and are associated with large errors which prevent an accurate determination. For $R_0(\text{Hg})$ the 3/2 power dependence is in very good agreement for the low Hg concentration experiments (Figure 16).

By keeping the absorbed light intensity I_{abs} constant while changing the initial mercury concentration $[\text{Hg}]_0$, we deduce from our mechanism (equation VII) that $R_0(\text{Hg})$ should be independent of $[\text{Hg}]_0$. However, this is not completely exemplified by our experiments, since a double logarithmic plot $\ln(R_0(\text{Hg}))$ vs $\ln([\text{Hg}]_0)$ yields a slope of 0.3 ± 0.1 (Figure 17). For $[\text{Hg}]_{\text{ss}}$ we derive the following relation under the condition of constant absorbed light intensity:

$$[\text{Hg}]_0/[\text{Hg}]_{\text{ss}} = 1 + \frac{\text{const}}{[\text{Hg}]_0} \quad (\text{IX})$$

A plot of the experimental data according to IX yields a straight line with an intercept of 2.1 ± 0.3 (Figure 17), rather than 1.0. The discrepancy between predicted and experimental result is in large parts due to the assumption of a linear dependence of I_{abs} on $[\text{Hg}]$.

It remains to be shown that the quantity const in eq VII has the same value in all three relations $R_0(\text{Hg})$ versus $I_0^{3/2}$, $[\text{Hg}]_0^{3/2}$, and $1/[\text{H}_2]$. The slope of the straight line in the last case (Figure 14) amounts to $m = \text{const } I_0^{3/2} [\text{Hg}]_0^{3/2} = (2.92 \pm 0.07) \times 10^{30} \text{ cm}^{-6} \text{ s}^{-1}$. With $I_0 = (3.60 \pm 0.11) \times 10^{13} \text{ cm}^{-3} \text{ s}^{-1}$ and $[\text{Hg}]_0 = (1.68 \pm 0.13) \times 10^{12} \text{ cm}^{-3}$, we arrive at $\text{const} = (6.2 \pm 0.8) \times 10^{-9} \text{ cm}^3 \text{ s}^{1/2}$. In the case of the I_0 dependence we obtain $\text{const} = (5.3 \pm 0.3) \times 10^{-9} \text{ cm}^3 \text{ s}^{1/2}$, whereas in the case of the $[\text{Hg}]_0$ dependence $\text{const} = (5.2 \pm 0.3) \times 10^{-9} \text{ cm}^3$

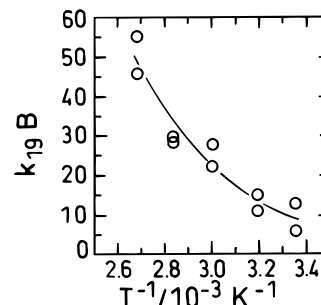


Figure 18. Arrhenius plot for $k_{19}B$.

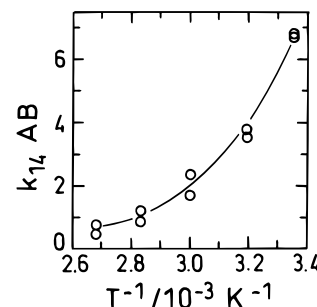


Figure 19. Arrhenius plot for $k_{14}AB$.

$\text{s}^{1/2}$. Taking the weighted mean of these three values yields

$$\text{const} = \frac{k_{14} k_4 (k_4 + 2k_5)^{1/2}}{k_{15} (k_4 + k_5)^{3/2}} \frac{\kappa^{3/2}}{(2(k_{10} + k_{11}))^{1/2}} = (5.3 \pm 0.2) \times 10^{-9} \text{ cm}^3 \text{ s}^{1/2} \quad (\text{X})$$

From (X) we can derive an approximate value for k_{14}/k_{15} . The rate constants k_4 , k_5 ,³ and k_{10} , k_{11} ²⁵ are known, only κ is not a very well-defined quantity which depends on the experimental conditions. From our own absorption measurements¹⁰ we derive a value of $\kappa \approx 5 \times 10^{-13} \text{ cm}^3$. From this it follows that

$$k_{14}/k_{15} = 1.2 \times 10^5$$

With the known rate constant for (15), $k_{15} = 3 \times 10^{-16} \text{ cm}^3 \text{ s}^{-1}$,²² we obtain a value of $k_{14} = 3.7 \times 10^{-11} \text{ cm}^3 \text{ s}^{-1}$, which has the correct order of magnitude for a radical combination reaction.

From the experiments in Table 1 it is also possible to derive a value for k_{19} . The product $\alpha^2\beta$ contains only k_{19} as an unknown rate constant

$$\alpha^2\beta = k_{19}B = k_{19} \left(\frac{k_4 + 2k_5}{k_4 + k_5} \frac{1}{2(k_{10} + k_{11})} \right)^{1/2} I_0^{1/2} \kappa^{1/2} \quad (\text{XI})$$

With the values for α and β given in Table 1, the value for κ , and the known rate constants, we arrive at a value of $k_{19} = (1.1 \pm 0.2) \times 10^{-13} \text{ cm}^3 \text{ s}^{-1}$ from the intensity dependence experiments. Similarly, the H₂ dependence yields $k_{19} = (1.3 \pm 0.3) \times 10^{-13} \text{ cm}^3 \text{ s}^{-1}$. From the $[\text{Hg}]_0$ dependence experiments a value of $k_{19} = (1.3 \pm 1.1) \times 10^{-13} \text{ cm}^3 \text{ s}^{-1}$ is obtained, which is in good agreement with the above results, however, with a larger uncertainty. The value of about $1 \times 10^{-13} \text{ cm}^3 \text{ s}^{-1}$ for a hydrogen abstraction reaction by an alkyl radical at room temperature is rather large, suggesting that the C₂H₅Hg-H bond energy is quite weak. The temperature dependence of $\alpha^2\beta$ can be mainly attributed to reaction 19. From Figure 19 we derive an activation temperature of $2500 \pm 300 \text{ K}$ for k_{19} . These results together with the value for k_{19} yields an A factor $\log(A(19)/\text{cm}^3 \text{ s}^{-1}) = -9.3 \pm 0.8$. This value is too large, but

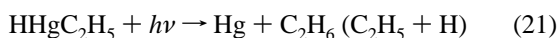
taking into account the complex analysis and the large errors involved, the result does not argue against the proposed mechanism.

Combining α and β in the following way

$$\beta(1 - \alpha^2) = k_{14}AB \quad (\text{XII})$$

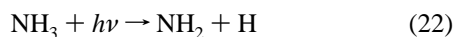
provides a quantity which contains only one rate constant, namely, k_{15} , with an appreciable temperature dependence. Because k_{15} is part of the denominator, we expect a negative activation energy when plotting $\ln(k_{14}AB)$ vs $1/T$. This is in fact the case, and from Figure 19 we derive an activation energy for reaction 15, $E_a(15) = 29.9 \pm 1.7$ kJ/mol. This value is in good agreement with the value given in ref 22 for the collision-induced decomposition of HgH by H₂.

A few reactions have to be added to the suggested mechanism to explain the experimental results in Tables 2 and 3. The increased rate of Hg formation when the sample is irradiated with 206 nm radiation can be rationalized by a direct photolytic decomposition of HHgC₂H₅.



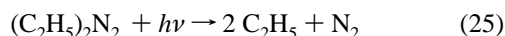
From Figure 12 it can be deduced that the absorption cross section for 206 nm photons is $\sigma \approx 3 \times 10^{-17}$ cm² taking into account $I_0(\lambda = 206 \text{ nm}) = 4.2 \times 10^{13}$ cm⁻³ s⁻¹ and $d = 6$ cm. This result agrees with the spectroscopic properties of mercury compounds. HgH₂ absorbs at 193 nm²⁶ but not at 254 nm. The maximum of the first absorption band of (CH₃)₂Hg is located at ~ 200 nm, the cross section at the maximum amounts to 3×10^{-17} cm².^{27,28} The absorption maximum of (C₂H₅)₂Hg is slightly shifted toward longer wavelengths.²⁹

Addition of NH₃ to our standard reaction system Hg/H₂/C₂H₄ has no effect. However, simultaneous photolytic decomposition of NH₃ leads to a substantial reduction of the stationary HHgC₂H₅ concentration. This can be explained by the three reactions



The two photolysis products of NH₃, H, and NH₂ have opposing effects with respect to the stationary concentration of HHgC₂H₅. The H atoms form mainly C₂H₅ radicals which favor HHgC₂H₅ formation via reaction 14 while NH₂ radicals have the opposite effect: reaction 24 directly affects the concentration of the mercury compound, while reaction 23 reduces the HgH and C₂H₅ radicals which are precursors to the mercury compound. Computer simulations suggest that the rate constant for reaction 24 is larger than k_{19} by approximately a factor of 2.

For the experiments given in Table 3 the photolytic decomposition of (C₂H₅)₂N₂



is essential for the formation of HHgC₂H₅. Without the simultaneous irradiation of the Hg/H₂/(C₂H₅)₂N₂ system with 254 and 206 nm light, no mercury compound is formed. The absorbed light intensity of the two light sources is roughly the same, and we expect similar rates of formation for HgH and C₂H₅, as in the 254 nm/Hg/H₂/C₂H₄ system. In contrast to the last system, there exists no large sink for the H atoms, like C₂H₄, and they will therefore react with HgH and C₂H₅, inhibiting the formation of HHgC₂H₅. This explains qualitatively the much

smaller rate of formation of HHgC₂H₅ in the 254 nm/Hg/H₂/(C₂H₅)₂N₂/206 nm system (Figure 13) compared to the 254 nm/Hg/H₂/C₂H₄ system (Figure 2).

We have also addressed the question whether the proposed reactions 17 and 19 can be directly demonstrated. If these two reactions are of any importance, then the product ratio [C₂H₆]/[C₄H₁₀] should be different in the experiments where the C₂H₅ radicals are generated by direct photochemical or thermal means and in experiments where they are generated in a system such as Hg/H₂/C₂H₄. Direct photolysis of (C₂H₅)₂N₂ at 366 nm yielded a [C₂H₆]/[C₄H₁₀] ratio of 0.124 ± 0.005 , while in the other system a value of 0.16 ± 0.01 has been found.

Conclusion

In the Hg-sensitized photolysis of H₂ in the presence of ethylene, as well as in the presence of other alkenes¹⁰ and in the Hg-sensitized photolysis of silanes^{9,10} or alkanes,¹⁰ it was observed that the sensitizer is consumed under formation of a metastable mercury compound. The experiments presented here show that HgH and C₂H₅ or more generally HgH and a radical are involved in the formation of this metastable compound. Concerning the structure of this compound, we have made the simplest assumption, namely, that it results directly from the combination of HgH with C₂H₅. Proof in the form of a mass spectrometric experiment failed. Indirect support for the suggested structure comes from more recent publications.^{30–34} In these works various organomercury hydrides have been prepared and characterized, a type of Hg compound which was thought to be unstable. Of importance to us is the finding that HHgCH₃ decomposes slowly at room temperature.³⁰

What are the consequences of this hitherto overlooked effect?

(i) If a low sensitizer concentration is chosen, e.g., to achieve a more uniform absorption of the resonance radiation, a systematic error in the quantum yield may result.

(ii) Disproportionation to recombination ratios of radicals will be too high, as demonstrated above.

(iii) This is a sensitive method to show the formation of HgH in the photochemical reaction between an excited Hg atom and a substrate.

References and Notes

- (1) von Büнау, G.; Wolff, T. *Photochemie*; VCH: Weinheim, 1987.
- (2) Cundall, R. B.; Palmer, T. F. *J. Chem. Soc., Faraday Trans.* **1960**, 56, 1211.
- (3) Callear, A. B.; McGurk, J. C. *J. Chem. Soc., Faraday Trans.* **1972**, 68, 289.
- (4) Gaydon, A. G. *Dissociation Energies and Spectra of Diatomic Molecules*; Chapman and Hall: London, 1968.
- (5) Wyrsh, D.; Wendt, H. R.; Hunziker, H. E. *Ber. Bunsen-Ges. Phys. Chem.* **1974**, 78, 204.
- (6) Gunning, H. E.; Strausz, O. P. *Adv. Photochem.* **1963**, 1, 209.
- (7) Cartland, H. E.; Pimentel, G. C. *J. Phys. Chem.* **1986**, 90, 1822; **1986**, 90, 5485.
- (8) Breckenridge, W. H. *J. Phys. Chem.* **1996**, 100, 14840.
- (9) Kerst, C.; Potzinger, P.; Wagner, H. G. *J. Photochem. Photobiol. A: Chem.* **1995**, 92, 141.
- (10) Lein, I. Diplomarbeit, Universität Göttingen, 1995.
- (11) de Maré, G. R. *J. Photochem.* **1977**, 7, 101.
- (12) Cvetanovic, R. J.; Falconer, W. E.; Jennings, K. R. *J. Chem. Phys.* **1961**, 35, 1225.
- (13) Martin, R. M.; Willard, J. E. *J. Chem. Phys.* **1964**, 40, 2999.
- (14) Ahmed, M.; Potzinger, P.; Wagner, H. G. *J. Photochem. Photobiol. A: Chem.* **1995**, 86, 33.
- (15) Groth, W. E.; Schurath, U.; Schindler, R. N. *J. Phys. Chem.* **1968**, 72, 3914.
- (16) McCaffrey, J. G.; Parnis, J. M.; Ozin, A.; Breckenridge, W. H. *J. Phys. Chem.* **1985**, 89, 4945.
- (17) Legay-Sommaire, N.; Legay, F. *Chem. Phys. Lett.* **1993**, 207, 123.
- (18) Legay-Sommaire, N.; Legay, F. *Chem. Phys. Lett.* **1994**, 217, 97.
- (19) Greene, T. M.; Brown, W.; Andrews, L.; Downs, A. J.; Chertihin, G. V.; Runeberg, N.; Pyykkö, P. *J. Phys. Chem.* **1995**, 99, 7925.

- (20) Bernier, A.; Millie, P. *J. Chem. Phys.* **1988**, 88, 4843.
- (21) Callear, A. B. *Chem. Rev.* **1987**, 87, 335.
- (22) Oka, K.; Cvetanovic, R. J. *J. Chem. Phys.* **1978**, 68, 4391.
- (23) Callear, A. B.; Hedges, R. E. M. *J. Chem. Soc., Faraday Trans.* **1970**, 66, 615.
- (24) Wardell, J. L. In *Comprehensive Organometallic Chemistry*; Wilkinson, G., Stone, F. G. A., Abel, E. W., Eds.; Pergamon: Oxford, 1982; Vol II, p 863.
- (25) Arthur, N. L. *J. Chem. Soc., Faraday Trans. 2* **1986**, 82, 1057.
- (26) Legay-Sommaire, N.; Legay, F. *J. Phys. Chem.* **1995**, 99, 16945.
- (27) Chen, C. J.; Osgood, R. M. *J. Chem. Phys.* **1984**, 81, 327.
- (28) Ibuki, T.; Hiraya, A.; Shobatake, K. *J. Chem. Phys.* **1990**, 92, 2797.
- (29) Thompson, H. W.; Linnett, J. W. *Proc. R. Soc. London Ser. A* **1936**, 156, 108.
- (30) Devaud, M. *J. Organomet. Chem.* **1981**, C27, 220.
- (31) Craig, P. J.; Mennie, D.; Needham, M.; Oshah, N.; Donard, O. F. X.; Martin, F. *J. Organomet. Chem.* **1993**, 447, 5.
- (32) Craig, P. J.; Garraud, J.; Laurie, S. H.; Mennie, D.; Stojak, G. H. *J. Organomet. Chem.* **1994**, 468, 7.
- (33) Kwetkat, K.; Kitching, W. *J. Chem. Soc., Chem. Commun.* **1994**, 345.
- (34) Craig, P. J.; Needham, M. I.; Stojak, G. H.; Symons, M.; Teesdale-Spittle, P. *J. Chem. Soc., Dalton Trans.* **1996**, 153.